Materials Science in Semiconductor Processing 66 (2017) 144–148

Contents lists available at ScienceDirect

Materials Science in Semiconductor Processing

journal homepage: www.elsevier.com/locate/mssp

Presence of NaI in PEO/PVdF-HFP blend based gel polymer electrolytes for fabrication of dye-sensitized solar cells

Negar Zebardastan, M.H. Khanmirzaei, S. Ramesh*, K. Ramesh

Centre for Ionics University of Malaya, Department of Physics, Faculty of Science, University of Malaya, 50603 Kuala Lumpur, Malaysia

ARTICLE INFO

Keywords:
PEO
PVdF-HFP
NaI
Gel polymer electrolyte
Dye-sensitized solar cell

ABSTRACT

Poly(vinylidene fluoride-co-hexafluoro propylene) copolymer (PVdF-HFP) and polyethylene oxide (PEO) blend gel polymer electrolytes (GPEs) containing ethylene carbonate (EC) and propylene carbonate (PC) as solvent with different concentrations of sodium iodide (NaI) salt are prepared. Effect of sodium iodide (NaI) on the gel polymer electrolyte system is investigated by using electrochemical impedance spectroscopy (EIS), temperature-dependence ionic conductivity, X-ray diffraction (XRD) and FTIR studies. The highest ionic conductivity value for the gel polymer electrolytes are 6.38 mS cm^{-1} in the presence of 100 wt% of sodium iodide (NaI) salt with respect to weight of PEO/PVdF-HFP polymer blend. The temperature-dependent ionic conductivity study indicates that the gel polymer electrolyte system follows the Arrhenius model. Dye-sensitized solar cells (DSSCs) are fabricated using gel polymer electrolytes and tested under Sun simulator. The highest energy conversion efficiency value of 5.67% is obtained after the addition of 100 wt% of sodium iodide (NaI) salt.

1. Introduction

Using different types of materials to prepare photo-anode or counter electrodes for the fabrication of dye-sensitized solar cells are one of the ways to improve the performance of dye sensitized solar cell (DSSC) [1–3]. Various researches have been conducted in the effort to increase the performance of dye-sensitized solar cells (DSSC) using the gel polymer electrolytes [4–8]. Gel polymer electrolyte (GPE) is very promising for providing a safe and high conductive polymer electrolyte system for fabrication of energy storage devices such as solar cell, battery and supercapacitor [9–11]. DSSCs can be prepared using natural, cost effective and environmentally friendly materials such as biopolymers [12]. PEO and PVdF-HFP blend polymer is a very good choice as a host polymer for preparation of high conductive gel polymer electrolyte due to the high electro-negativity of Fluorine and also the high interaction between the C-O-C and CF_2 groups of PEO and PVdF-HFP respectively [13–15]. Research has shown that the presence of NaI salt in the system increases the ionic conductivity of the gel polymer electrolyte by providing more cations as charge carriers and also shows the improvement in the performance of DSSC by contributing in I^-/I_3^- redox couple [16–22]. In this research the gel polymer electrolytes were prepared and the effect of the NaI salt into the system was investigated. The dye sensitized solar cells (DSSCs) were fabricated using the PEO/PVdF-HFP based gel polymer electrolyte by incorporation of different concentration of NaI salt into the system to study the photovoltaic performance of the DSSCs.

2. Experimental

2.1. Materials

Polyethylene oxide (PEO) (average Mw ~6×10^5 g mol^{-1}, powder), poly (vinylidene fluoride-co-hexafluoropropylene) (PVdF-HFP) (average Mw ~4×10^5 g mol^{-1}, pellets), ethylene carbonate (EC) (Mw = 88.06 g mol^{-1}), propylene carbonate (PC) (Purity > 99.7%), sodium iodide (NaI) (powder, Purity > 99%) and Iodine (I_2) (pearl, Purity > 99.8%), were purchased from Sigma-Aldrich. PEO, PVdF-HFP, EC, PC, NaI and I_2 were used without any further purification. NaI salt was dried in oven for 2 h before use.

2.2. Preparation of gel polymer electrolyte

PEO/PVdF-HFP:NaI:I_2 gel polymer electrolytes were prepared using the heating and stirring process. At first, The optimized and fixed weight percentage (wt%) of 40:60 were obtained for the PEO and PVdF-HFP polymers, respectively where the whole weight of these two polymers were 0.7 g. In the first step of preparation of gel polymer electrolytes, 8 g of clear mixture of EC and PC plasticizers were obtained with the weight ratio of 1:1 by stirring under 60 °C. Then, 20, 40, 60, 80 and 100 wt% of NaI salt (with respect to the total weight of PEO and PVdF-HFP polymers) were added to the EC:PC mixture by stirring for 2 h at the same temperature. Then PEO and PVdF-HFP polymers (40:60 wt%) were

* Corresponding author.
E-mail addresses: khanmirzaei2@gmail.com (M.H. Khanmirzaei), rameshtsubra@gmail.com (S. Ramesh).

http://dx.doi.org/10.1016/j.mssp.2017.04.016
Received 16 September 2016; Received in revised form 14 April 2017; Accepted 18 April 2017
Available online 26 April 2017

dissolved into the EC:PC:NaI mixture by stirring under 100 °C overnight. Lastly Iodine (I_2) (1/10 M ratio of NaI), was added and dissolved into the homogeneous solution of PEO/PVdF-HFP:NaI under 80 °C.

2.3. Dye-sensitized solar cell (DSSC) fabrication

The photo-anode electrode for fabrication of dye-sensitized solar cells were prepared by coating 2 different layers of TiO_2 by spin coating (2 s at 1000 rpm and 60 s at 2350 rpm) and doctor blade methods, respectively, on the Fluorine doped tin oxide (FTO) glass substrates and in each step the coated layer were sintered at 450 °C for 30 min. The TiO_2 paste for the first layer were prepared by grinding 0.5 g of TiO_2 (P90) nanopowder in 2 ml HNO_3 (PH = 1) and for the second layer, 0.5 g of TiO_2 (P25) was ground with 2 ml of HNO_3 (pH = 1), one drop of Triton X-100 and 0.1 g carbowax in the agate mortar. Furthermore the FTO glass substrate with two different coated layers of TiO_2 was soaked in the N719 dye solution for one whole day and dried to complete the processes of photo-anode preparation. Gel polymer electrolytes were sandwiched between photo-anodes and counter electrodes for subsequent characterizations as illustrated in Fig. 1.

2.4. Characterization method

2.4.1. Electrochemical impedance spectroscopy (EIS)

The ionic conductivity in ambient temperature and temperature-dependent ionic conductivity studies of the GPEs were carried out using the 3532-50 LCR HITESTER spectrometer. GPEs were cast into the stainless steel cell with a fixed thickness of 0.2828 cm and a fixed voltage of 0.01 V were applied over the cell in the frequency range between 50 Hz and 5 MHz. The ionic conductivity (σ) for all the GPEs was calculated by the following equation:

$$\sigma = \frac{L}{R_b A} \quad (1)$$

where σ is the ionic conductivity (S cm^{-1}), L is the thickness of the sample (in cell), R_b is the bulk resistance (Ω) obtained from the Cole-Cole plots of the gel polymer electrolytes from EIS results and A is the contacting area of the blocking stainless steel electrodes.

For temperature-dependent ionic conductivity studies, the stainless steel cell was filled with the gel polymer electrolytes each time and placed in the oven; the door was closed and the relevant Cole-Cole plot was obtained at different temperatures from 30 to 100 °C.

2.4.2. X-ray diffraction (XRD)

The XRD patterns of GPEs were recorded using PANalytical Empyrean diffractometer (45 kV, 40 mA) with wavelength of λ = 1.540600 Å for 2θ range of 5–80° at ambient temperature.

2.4.3. Fourier transform infrared spectroscopy (FTIR)

The FTIR spectra of all GPEs were obtained by using the Attenuated Total Reflection (ATR)-FTIR Perkin Elmar spectrum 400 spectrometer to investigate the interaction between materials in the system. In order to obtain the FTIR spectra for all the GPEs a small amount of gel polymer electrolyte was simply placed on the surface of ATR crystal of the spectrometer each time.

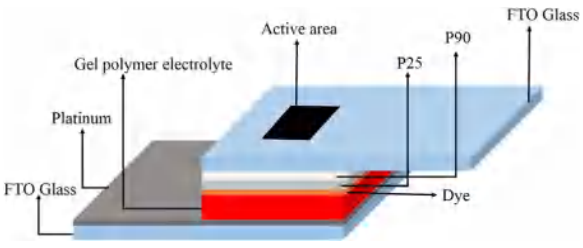

Fig. 1. Illustration of dye-sensitized solar cells fabricated in this work.

Table 1
Designation with the corresponding ionic conductivity and activation energy values of the gel polymer electrolytes.

GPE designation	NaI content (wt%)	σ (mS cm^{-1})	E_a (eV)
PP-NaI-20	20	2.29 ± 0.09	0.117 ± 0.006
PP-NaI-40	40	3.78 ± 0.08	0.114 ± 0.004
PP-NaI-60	60	5.02 ± 0.07	0.108 ± 0.001
PP-NaI-80	80	5.82 ± 0.09	0.105 ± 0.002
PP-NaI-100	100	6.38 ± 0.08	0.098 ± 0.007

2.4.4. Characterization of dye-sensitized solar cell (DSSC)

A multi-channel Autolab (PGSTAT30) potentiostat workstation at a scan rate 100 mV s^{-1}, a stop potential 800 mV and a step potential of 5 mV was used to obtain J-V characteristic curves of GPEs. The photo-voltaic performance of DSSCs was investigated by placing the fabricated DSSCs under the simulated Sun light using Keithley 2400 electrometer with incident light power intensity of 1000 W m^{-2}. Black silicone tape was used to create and control the active area of dye-sensitized solar cells. Three DSSCs were fabricated each time to investigate the photo-voltaic performance of DSSCs based on the PP-NaI-20, PP-NaI-40, PP-NaI-60, PP-NaI-80 and PP-NaI-100.

3. Results and discussion

3.1. Ionic conductivity studies (EIS)

Table 1 shows the designation for the gel polymer electrolytes and the relevant ionic conductivity values. Fig. 2 shows the variation of the ionic conductivity of the gel polymer electrolytes in presence of different concentration of sodium iodide (NaI) from 0 to 100 wt%. Improvements in the ionic conductivity values can be observed in the presence of the NaI salt where the highest ionic conductivity value of 6.38 mS cm^{-1} after incorporation of 100 wt% of NaI salt is obtained. The contribution of NaI in the system increases the charge carriers where I^- ions from the dissociation of NaI in the system can be considered as a source of the I^-/I_3^- redox couple next to the Iodine (I_2).

3.2. Temperature-dependent ionic conductivity studies

The ionic conductivity of GPEs was measured with different temperature from 303 K to 373 K and the results were demonstrated in Fig. 3. Based on the results, increasing the temperature causes an increment in the ionic conductivity value of the gel polymer electrolytes. Increase in the ionic conductivity with temperature shows the fast

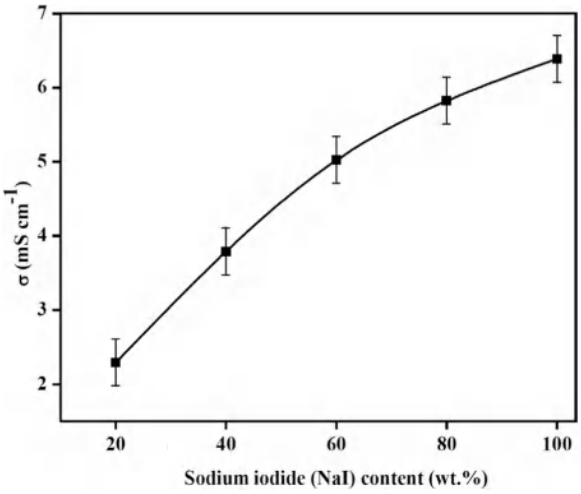

Fig. 2. Variation of ionic conductivity in presence of different concentrations of NaI salt in the gel polymer electrolyte system.

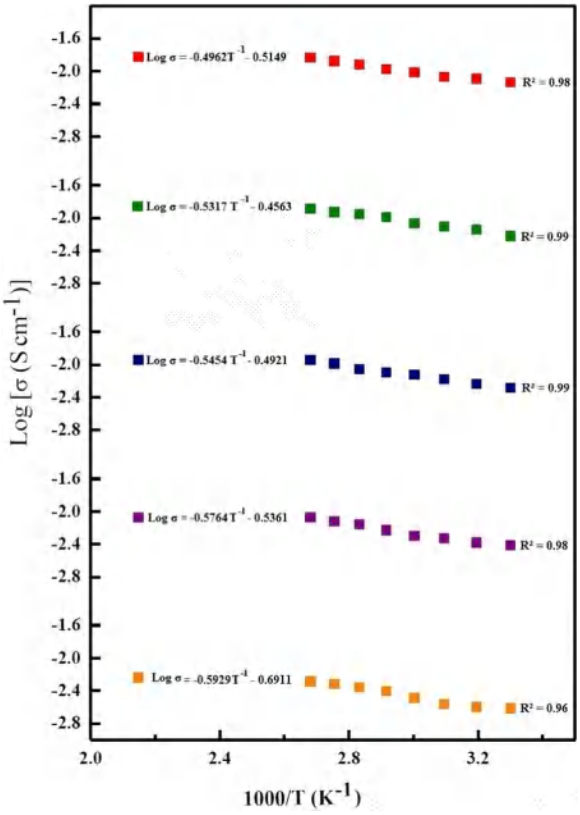

Fig. 3. Temperature-dependent ionic conductivity results PP-NaI-20 (down), PP-NaI-40, PP-NaI-60, PP-NaI-80 and PP-NaI-100 (top) gel polymer electrolytes.

mobility of ions in the system and it may be due to the increasing amorphous phase of the host polymers where the PEO and PVDF-HFP has a low glass transition temperature especially compared with the EC and PC plasticizers [23,24]. The thermal ionic conductivity behavior of all the gel polymer electrolytes shows an almost straight line with the regression values ~1 according to the Arrhenius thermal activated model as shown in the equation below

$$\sigma = \sigma_0 \exp\left[\frac{-Ea}{kT}\right] \quad (2)$$

where σ (S cm^{-1}) is the ionic conductivity, σ_0 (S cm^{-1}) is the pre-exponential factor, E_a (ev) is the activation energy, k (eV K^{-1}) is the Boltzmann constant and T is the temperature in Kelvin. Table 1 shows the calculated activation energies for all the gel polymer electrolytes with different concentration of NaI content. The activation energy value decreases with increasing the concentration of NaI salt in the system and it starts to decrease from 0.117 eV for the gel polymer electrolyte with 20 wt% NaI content to 0.098 eV, which is the lowest activation energy value and corresponds to the highest conducting gel polymer electrolyte with 100 wt% NaI content.

3.3. XRD study

Fig. 4 represents the XRD pattern for pure polymers (PEO and PVdF-HFP), PEO/PVdF-HFP polymer blend and NaI salt. The XRD patterns for PEO shows two sharp peaks at 2θ = 19° and 23°. The XRD patterns for PVdF-HFP shows semicrystalline nature of this copolymer [24] with crystalline sharp peaks at 2θ = 20°, 29° and 38°. The XRD patterns for PEO/PVdF-HFP blend system show the amorphous morphology, which proves the complete blending of these polymers in the system and as a result increasing amorphous phase by preventing the re-crystallization in the system. The NaI XRD results in Fig. 4 shows highly crystalline nature of this salt. The crystalline peaks of the NaI salt do not appear in the XRD results of the PP-

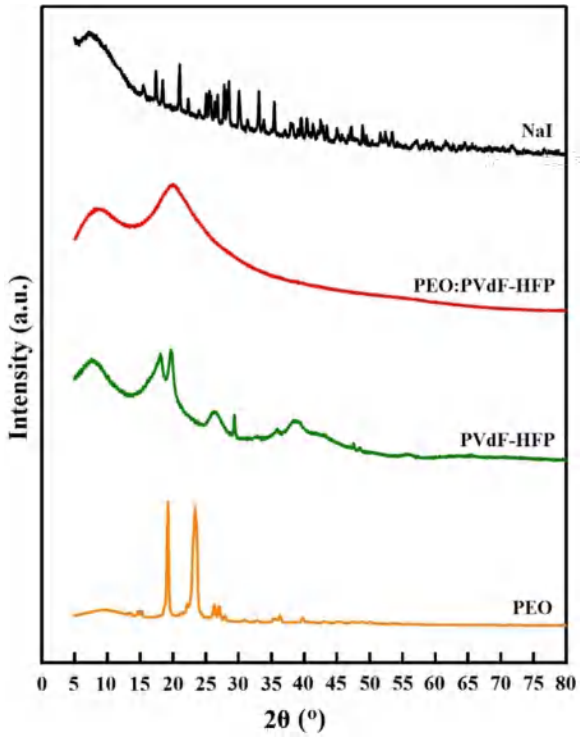

Fig. 4. XRD patterns for NaI salt, PEO, PVdF-HFP and PEO/PVdF-HFP polymers.

NaI-20, PP-NaI-40, PP-NaI-60, PP-NaI-80 and PP-NaI-100 due to the full dissolution of NaI into the gel polymer electrolyte system. Based on Fig. 5 the semicrystalline peak in PEO/PVdF-HFP blend polymer system decreases in intensity in the presence of 20 wt% NaI salt and it continues to decrease with the addition of NaI salt up to 100 wt% due to the complexation between NaI and the other materials in the system [25].

3.4. Fourier transform infrared (FTIR) studies

The interaction between PEO, PVdF-HFP and NaI salt in the gel polymer electrolyte system were investigated by using the FTIR analysis. Fig. 6 shows FTIR spectra for Pure PEO, PVdF-HFP and pure NaI salt, and Table 2 represents the band assignments of the pure PEO, PVDdF-HFP and NaI salt. The interaction between NaI salt and the host polymers can be understood by investigating any changes in these characteristic peaks in the combined FTIR spectra for all the gel polymer electrolytes with different amounts of NaI content from 20 to 100 wt%. The FTIR spectra for GPEs with different NaI contents are represented in Fig. 7. The characteristic peak of NaI at 3414 cm^{-1} is shifted to 3559, 3567, 3559, 3560 and 3579 cm^{-1} in PP-NaI-20, PP-NaI-40, PP-NaI-60, PP-NaI-80 and PP-NaI-100, respectively, after NaI is complexed with PEO and PVdF-HFP polymer blends. These changes in the NaI characteristic band may be due to the interaction between Na^+ cation and the Fluorine in the PVdF-HFP polymer when the NaI dissolves in the gel polymer electrolyte system and dissociate into I^- anion and Na^+ cation. Moreover, the peak at 2879 cm^{-1} in PEO and two peaks at 3026 and 2985 cm^{-1} in PVdF-HFP, after blending and complexation with NaI salt, are shifted to lower wavenumbers in PP-NaI-20, PP-NaI-40, PP-NaI-60, PP-NaI-80 and PP-NaI-100 where the values are mentioned in Fig. 7. The wavenumber at 1554 cm^{-1} in the PP-NaI-20 spectrum is due to the interaction between the CH_2 scissoring band of PEO and C-F stretching vibration band of PVdF-HFP polymers which increase to 1556 cm^{-1} by increasing the concentration of NaI salt up to 100 wt%. The wavenumber at 848 cm^{-1} is increased to 849 cm^{-1} due to the interaction of NaI salt with the mixed mode of CH_2 rocking of PVdF-HFP and CH vibration of PEO polymers. The peak at 772 cm^{-1} in the PP-NaI-20 spectrum is shifted to 773 cm^{-1} in the PP-NaI-100 spectrum due to the interaction between the CF_3 stretching vibration

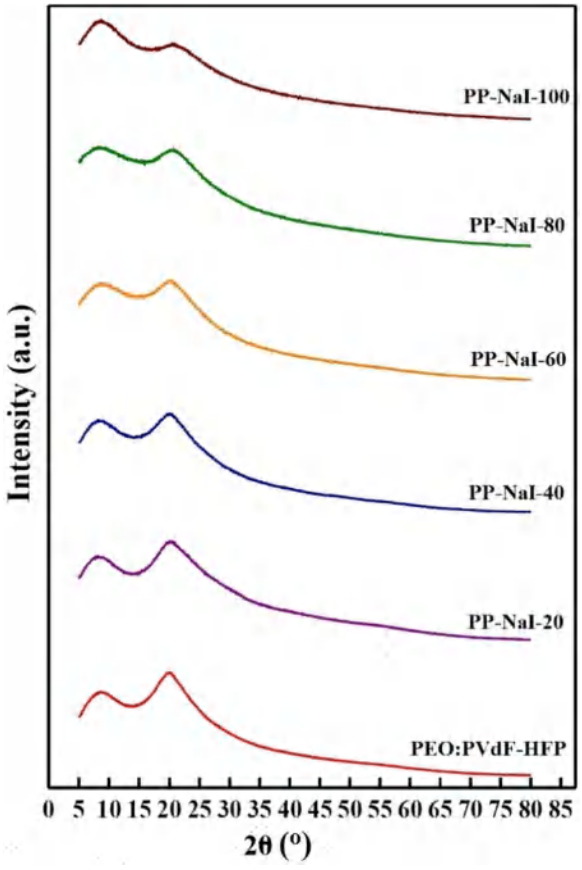

Fig. 5. XRD patterns for PEO/PVdF-HFP and PP-NaI-20, PP-NaI-40, PP-NaI-60, PP-NaI-80 and PP-NaI-100 gel polymer electrolytes.

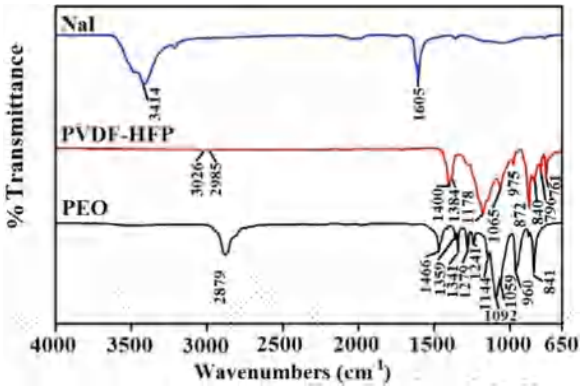

Fig. 6. FTIR spectra of pure PEO, PVdF-HFP and NaI.

Table 2
The FTIR absorption bands for the pure polymers and NaI salt that were used in preparation of the gel polymer electrolytes.

Material	Wavenumber (cm^{-1})	Peak assignments	References
Pure PEO	2879	CH band	[26–28]
	1466	CH_2 scissoring	
	1359, 1059	C-O-C stretching	
	1341	Waging vibration	
	1279, 1241	C-O band	
	1144, 1092	C-O-C band	
	841	CH vibration	
Pure PVDF-HFP	3026, 2985	Symmetric and antisymmetric stretching vibration of CH_2	[29,30]
	1400	C-F stretching vibration	
	975	C-F stretching	
	872	Combined CF_2 and CC symmetricstretching vibrations	
	840	Mixed mode of CH_2 rocking	
	796	CF_3 stretching vibration	
	761	CH_2 rocking vibration	
NaI	1605,3414	The sodium iodide characteristic peaks	[31]

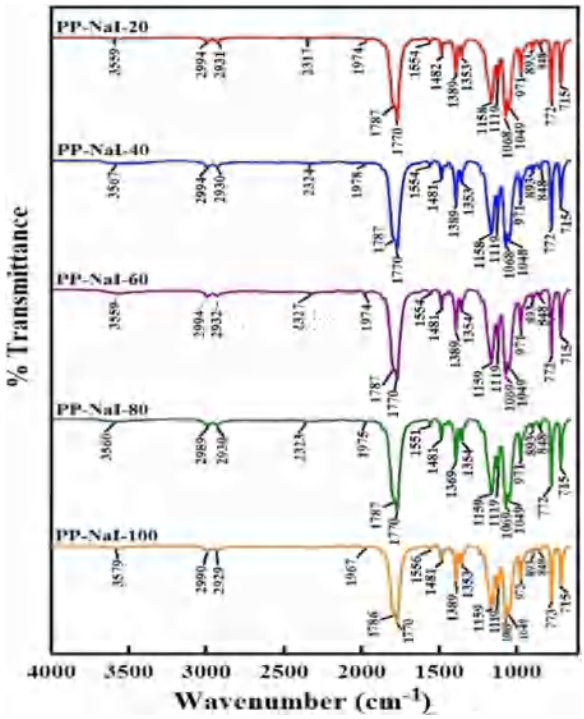

Fig. 7. FTIR spectra for PP-NaI-20, PP-NaI-40, PP-NaI-60, PP-NaI-80 and PP-NaI-100 GPEs.

of PVDF-HFP and NaI and the wavenumber at 893 cm^{-1} in the PP-NaI-20 spectrum decreased in intensity in the PP-NaI-100 spectrum due to the interaction between combined CF_2 and CC symmetric stretching vibrations of PVDF-HFP and addition of NaI. All the changes in the wavenumbers on increasing the amount of NaI salt in the gel polymer electrolyte system up to 100 wt% proves the interaction and complexation between the NaI salt and the other materials in the system.

3.5. Photovoltaic performance of dye sensitized solar cell (DSSC)

The J-V characteristic curves for all GPEs are represented in Fig. 8 and the effect of NaI salt on the efficiency of DCCSs fabricated by using PP-NaI-20, PP-NaI-40, PP-NaI-60, PP-NaI-80 and PP-NaI-100 gel polymer electrolytes were investigated. The efficiency (η) and the fill factor were calculated by using the following equations

$$\eta = \frac{J_{sc}.\ V_{oc}.\ FF}{P_{in}} \tag{3}$$

where J_{sc} (mA cm^{-2}) and V_{oc} (V) are the short-circuit current density and open-circuit voltage, respectively. Fill factor is defined by

$$FF = \frac{P_{max}}{J_{sc} V_{oc}} \tag{4}$$

where P_{max} (mW cm^{-2}) is the maximum power output of the solar cell. The photovoltaic performance of the fabricated DSSCs was analyzed under the Sun simulator with 100 (mW cm^{-2}) light power. Enhance-

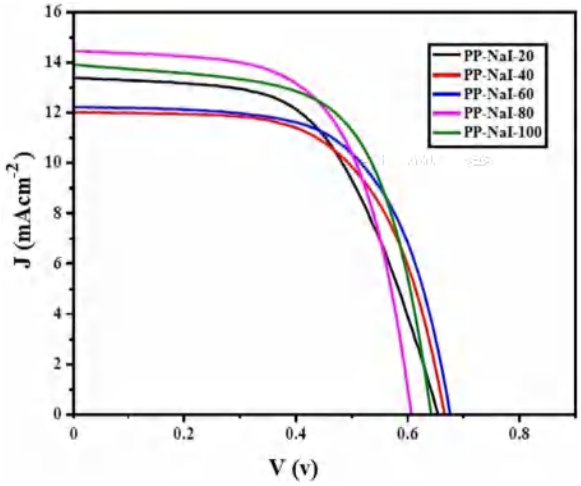

Fig. 8. J-V characteristic curves for the DCCSs fabricated using PP-NaI-20, PP-NaI-40, PP-NaI-60, PP-NaI-80 and PP-NaI-100 GPEs.

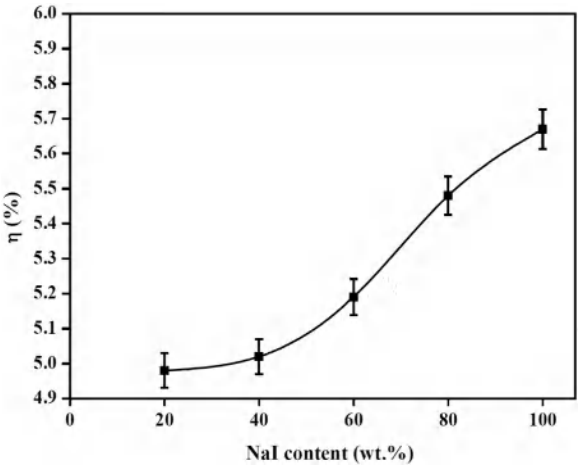

Fig. 9. Variation of efficiency with different concentrations of NaI salt.

Table 3
The values of the Photovoltaic parameters for the fabricated DSSCs by using PP-NaI-20, PP-NaI-40, PP-NaI-60, PP-NaI-80 and PP-NaI-100 GPEs.

Electrolyte	J_{sc} (mA cm^{-2})	V_{oc} (V)	FF (%)	Efficiency, η (%)
PP-NaI-20	13.39 ± 0.17	0.654 ± 0.001	56.90 ± 0.02	4.98 ± 0.05
PP-NaI-40	12.03 ± 0.10	0.665 ± 0.002	62.70 ± 0.06	5.02 ± 0.03
PP-NaI-60	12.22 ± 0.06	0.675 ± 0.003	62.90 ± 0.01	5.19 ± 0.06
PP-NaI-80	14.45 ± 0.21	0.600 ± 0.003	63.20 ± 0.03	5.48 ± 0.03
PP-NaI-100	13.93 ± 0.19	0.639 ± 0.001	63.70 ± 0.13	5.67 ± 0.06

ments in the energy conversion efficiency values of the DSSCs can be observed clearly in Fig. 9, with increasing NaI content in the gel polymer electrolyte system. All the photovoltaic parameter values of the fabricated DSSCs are represented in Table 3. The highest energy conversion efficiency value of 5.67% was obtained from using PP-NaI-100 gel polymer electrolyte with 100 wt% NaI salt content. The contribution of NaI salt in providing I^-/I^{3-} redox couples and also facilitation of the ion movements in the high conductive gel polymer electrolyte developed the performance of DSSC.

4. Conclusion

The PEO/PVdF-HFP blend polymer based gel polymer electrolytes with different amounts of NaI salt from 20 to 100 wt% were prepared and the dye-sensitized solar cells were fabricated using the gel polymer electrolytes prepared in this work. Increasing the ionic conductivity of the gel polymer electrolytes with increasing the NaI content in the system up to 100 wt% with respect to the amount of PEO and PVdF-HFP polymers were observed and the highest ionic conductivity of 6.38 mS cm^{-1} was achieved for PP-NaI-100 after incorporation of 100 wt% of NaI salt. The temperature-dependent ionic conductivity of all the gel polymer electrolytes proved the Arrhenius behavior and the activation energy value decreased up to 0.098 eV for PP-NaI-100. The XRD pattern for all the gel polymer electrolytes shows the semi-crystalline nature of the gel polymer electrolytes. Increasing the amount of NaI salt in the system proves the complexation between PEO/PVdF-HFP polymer blend and NaI salt in the system. The absorption peaks in the FTIR spectra show the shifting in the wavenumbers by increasing the NaI amount up to 100 wt% NaI salt, which proves the interaction between NaI salt and PEO/PVdF-HFP polymer blend in the system. The performance of all the fabricated dye-sensitized solar cells using PP-NaI-20, PP-NaI-40, PP-NaI-60, PP-NaI-80 and PP-NaI-100 GPEs were analyzed under the Sun simulator with 100 mW cm^{-2}. From the J-V results, the efficiencies were calculated. The dye-sensitized solar cell fabricated with PP-NaI-100 gel polymer electrolyte shows the highest efficiency value of 5.67%. PP-NaI-100 gel polymer electrolyte which was prepared in this work is a very good candidate for fabrication of high performance dye-sensitized solar cell for its unique features such as being highly conductive, safe for fabrication of dye-sensitized solar cell, simplicity of preparation and access to the materials and more importantly, for making high efficiency dye-sensitized solar cell.

Acknowledgements

This work is financially supported by Fundamental Research Grant Scheme (FP012-2015A), from Ministry of Education, Malaysia.

References

[1] H. Xu, G. Zhu, Mater. Lett. 171 (2016) 174–177.
[2] A.F. Kanta, A. Schrijnemakers, A. Decroly, Mater. Des. 95 (2016) 481–485.
[3] I. Iwantono, et al., Effect of Growth Solution Concentration on the Performance of Gallium Doped ZnO Nanostructures Dye Sensitized Solar Cells (DSSCs), 2016, 1712, p. 050024.
[4] T.M.W.J. Bandara, et al., J. Solid State Electrochem. 19 (8) (2015) 2353–2359.
[5] H.-T. Chou, et al., Microelectron. Reliab. 55 (11) (2015) 2174–2177.
[6] S.Y. Shen, et al., ACS Appl. Mater. Interfaces 6 (21) (2014) 18489–18496.
[7] J.E. Benedetti, et al., Ionics 21 (6) (2014) 1771–1780.
[8] M.H. Khanmirzaei, S. Ramesh, K. Ramesh, Sci. Rep. 5 (2015) 18056.
[9] C.-H. Tsao, P.-L. Kuo, J. Membr. Sci. 489 (2015) 36–42.
[10] Q. Wang, et al., J. Membr. Sci. 486 (2015) 21–28.
[11] J. Zhong, et al., Electrochim. Acta 166 (2015) 150–156.
[12] S.N.F. Yusuf, et al., RSC Adv. 6 (33) (2016) 27714–27724.
[13] K. Prabakaran, S. Mohanty, S.K. Nayak, RSC Adv. 5 (51) (2015) 40491–40504.
[14] K. Prabakaran, S. Mohanty, S.K. Nayak, J. Mater. Sci.: Mater. Electron. 26 (6) (2015) 3887–3897.
[15] K. Prabakaran, S. Mohanty, S.K. Nayak, Ceram. Int. 41 (9, Part B) (2015) 11824–11835.
[16] M.M. Noor, et al., Electrochim. Acta 121 (2014) 159–167.
[17] W.C. Tan, et al., J. Solid State Electrochem. 16 (6) (2011) 2103–2112.
[18] Z. Lan, et al., Electrochim. Acta 53 (5) (2008) 2296–2301.
[19] Z. Lan, et al., Sol. Energy 80 (11) (2006) 1483–1488.
[20] J.H. Kim, et al., Solid State Ion. 176 (5–6) (2005) 579–584.
[21] M.H. Khanmirzaei, S. Ramesh, K. Ramesh, Ionics (2015) 1–9.
[22] M.H. Khanmirzaei, S. Ramesh, K. Ramesh, Mater. Des. 85 (2015) 833–837.
[23] M.A.K.L. Dissanayake, et al., J. Solid State Electrochem. 20 (1) (2015) 193–201.
[24] N. Ataollahi, et al., Int. J. Electrochem. Sci. 7 (2012) 6693–6703.
[25] N.S. Rani, et al., Ionics 20 (2) (2013) 201–207.
[26] B.-R. Choi, S.-J. Park, S. Kim, J. Ind. Eng. Chem. 31 (2015) 352–359.
[27] S. Farheen, R.D. Mathad, Int. J. Adv. Sci. Technol. 81 (2015) 49–52.
[28] W. Na, et al., Electrochim. Acta 188 (2016) 582–588.
[29] S. Shalu, V.K. Singh, R.K. Singh, J. Mater. Chem. C 3 (28) (2015) 7305–7318.
[30] D. Saikia, A. Kumar, Eur. Polym. J. 41 (3) (2005) 563–568.
[31] J.F.B.Z. Abiddin, A.H. Ahmad, Conductivity Study and Fourier Transform Infrared (FTIR) Characterization of Methyl Cellulose Solid Polymer Electrolyte with Sodium Iodide Conducting Ion, 2015, 1675, p. 020026.